Ecosystem Health and Sustainability
A SCIENCE PARTNER JOURNAL

RESEARCH ARTICLE

Integrating Ecosystem Service Supply and Demand to Construct Regional Ecological Security Patterns

Ruyuan Hu[1,2,3†], Haiping Zhao[1,2,3†], Jia Yang[4], Mengmeng Gou[1,2,3*], Changfu Liu[1,2,3], Le Li[5], and Wenfa Xiao[1,2,3]

[1]Ecology and Nature Conservation Institute, Chinese Academy of Forestry, Beijing 100091, China. [2]Key Laboratory of Forest Ecology and Environment of Forestry and Grassland Administration, Beijing 100091, China. [3]Hubei Zigui Three Gorges Reservoir Forest Ecosystem Observation and Research Station, Zigui 443600, China. [4]College of Ecology and Environment, Central South University of Forestry and Technology, Changsha 410004, China. [5]Research Institute of Tropical Forestry, Chinese Academy of Forestry, Guangzhou 510520, China.

*Address correspondence to: goumm0243@126.com
†These authors contributed equally to this work.

Citation: Hu R, Zhao H, Yang J, Gou M, Liu C, Li L, Xiao W. Integrating Ecosystem Service Supply and Demand to Construct Regional Ecological Security Patterns. *Ecosyst. Health Sustain.* 2025;11:Article 0457. https://doi.org/10.34133/ehs.0457

Submitted 25 June 2025
Revised 15 August 2025
Accepted 26 November 2025
Published 12 December 2025

Integrating ecosystem services (ESs) into ecological security patterns (ESPs) provides a comprehensive framework for recognizing critical conservation areas and enhancing regional ecological security. However, previous studies are predominantly based on ES supply, while often not fully considering the supply–demand balance and its dynamic trends. This study proposed a comprehensive framework including comprehensive supply–demand ratio (CSDR), CSDR trend, total supply trend, and trade-off to revise ecological source recognition. Subsequently, ecological resistance surfaces were revised using land use and nighttime light data. Finally, corridors and strategic nodes were further recognized according to circuit theory to establish a comprehensive ESP. Selecting Three Gorges Reservoir Area as a research case, the results show that the ecological sources (18,232.59 km^2) are predominantly situated in the eastern regions and parts of the southern bank of the Yangtze River with high supply and low ecological risks and trade-off levels. The low value of the resistance surfaces is distributed consistently with ecological sources, and the high value of the resistance surfaces is distributed near the cities with high population density and demand. Two hundred sixty-six key ecological corridors and 195 pinch points connected the regions into an organic whole and barrier points, with an area of 285.96 km^2 overlapping with the potential corridors. These findings offer guidance for regional planning and sustainable development.

Introduction

Ecosystem services (ESs) are the benefits derived by humans from the ecosystems, which create a bridge to nature and social systems [1,2]. Ecological security means the state in which the ES supply capacity is in line with the demand for ES of human social and economic development [3]. Over the past few years, increased human activities and rapid socioeconomic development under climate change have induced widespread ecosystem function degradation, thereby effectively blocking the sustainable delivery of ESs to meet human societal needs [4]. Under these circumstances, the ecological security pattern (ESP) has appeared as an essential regulatory mechanism for optimizing spatial allocation and promoting supply–demand dynamical balance [5]. However, one of the major challenges in formulating effective ESP to secure ESs is the insufficient understanding about the perspective of supply–demand matches [6].

The construction of ESPs supports regional management by identifying and conserving critical ecological components [7]. Up to now, a main research paradigm, namely, "source recognition-resistance surface analysis-corridor pathway extraction", is mainly used to construct ESP [8]. Ecological sources are critical habitat patches vital for protecting the ecological security, as they are instrumental in mitigating ecosystem degradation, providing ESs, and preserving landscape integrity [9]. The recognition of ecological sources involves the direct selection of vital natural reserve [10] and a comprehensive assessment of ecological importance, including ecological risks, ES importance, and other related factors [11,12]. Ecological resistance surfaces indicate the degree of species' migration among different landscape patches, serving as a central step in recognizing ecological corridors [13]. Ecological corridors are predominantly pathways for the flow of energy and migration of species, enhancing connectivity among ecological source areas [3]. Ecological strategic nodes are divided into pinch and barrier points, both of which affect the landscape connectivity [14]. Recently, circuit theory has effectively employed the recognition of regional landscape connectivity and construction of ESPs [15]. Thus, the precise recognition of ecological sources is a critical prerequisite for constructing ESPs.

Ecological source is mainly identified by assessing ecological risk in this study, which serves as the inverse measure or function assumption of ecological security and helps classify risk levels [16]. However, current research on the recognition of ecological sources based on ecological risk still has notable limitations. Most studies have primarily concentrated on the ES supply capacity, but have ignored the relationships between human demand and nature supply [17]. As a result, ecological source areas tend to be concentrated only in supply-dominant regions [18], while areas with high human demand still face ecological risks due to insufficient supply and excessive resource exploitation [19]. Meanwhile, these studies predominantly emphasized only a few ESs, such as soil retention and water yield, while often ignoring the trade-offs among numerous ES supply [20]. When ESs exist trade-offs, enhancing the provision of one service often reduces the availability of other critical services [21]. Consequently, policy making and management practices that only focus on the enhancement of a single ES function, while overlooking its inherent trade-offs, may inadvertently compromise other services that are equally vital to human well-being [22]. Previous studies have integrated ES supply and demand to evaluate the spatial matching to assess risk, while they lack temporal dynamics, which limit their ability to capture shifts in supply–demand trends [16,23]. Moreover, the static interrelation between supply and demand does not account for the dynamic interactions within social-ecological systems. It is also difficult to quantify the lag of ecological risks owing to the rapid land use change and socioeconomic fluctuations, which is not possible to accurately recognize the ecological source regions and affect ESP construction, and further limit effective long-term guidance for sustainable ecological protection and management [24]. For instance, regions presently in a supply–demand equilibrium have shown a persistent decline in ES supply, indicating a potential risk of insufficient future supply and progressive ecosystem degradation [9]. Therefore, it is essential to assess ecological security so as to identify ecological sources and construct ESP that consider both supply–demand balances and temporal dynamics.

The balance of ES supply–demand is a vital precondition to guarantee ecological security [13]. Over the past few years, the supply–demand imbalance in Three Gorges Reservoir Area (TGRA) has caused a number of ecological issues, such as nonpoint pollution and soil erosion, which have become the major factors that threaten ecological security and restrict the region's socioeconomic growth in a sustainable manner [21,25]. Nevertheless, the supply–demand analysis of ESs has seldom been incorporated to participate in ESP construction. To fill this gap, TGRA was selected as a case study to (a) construct a novel framework to recognize ecological sources by simultaneously taking into account the status and trends of comprehensive supply–demand ratio (CSDR), trends of ES supply, and trade-offs of ES supply and (b) further identify resistance surfaces, corridors, and strategic nodes and formulate targeted policies for ecological management and restoration based on this established ESP.

Materials and Methods

Study area

TGRA (28°56′N to 31°44′N, 106°16′E to 111°28′E), with an area of 57,900 km^2, is situated in the upper and middle reaches of the Yangtze River and composed of 20 counties or districts across Chongqing City and Hubei Province (Fig. 1). Within TGRA, the topography is complex, with elevation ranging from 10 to 2,926 m above sea level. The eastern region is composed of a series of mountains, and the western region is mostly consisted of plains and hills. The main climatic characteristic belongs to the humid subtropical monsoon, owing to a temperature of 17 to 19 °C and an average yearly rainfall of 1,250 mm. Purple, brown, and yellow-brown soils are the mostly soil types, and forestland, cropland, and grassland are the predominant land cover [25].

TGRA, a classic ecologically fragile region in China, is influenced by multiple effects of nature and humans. The rapid construction process has greatly changed the original ecosystem structure and function, resulting in more vulnerability and complexity of the reservoir ecosystem with the ever-increasing population [26]. In response to these ecological problems, many ecological restoration and conservation policies have been enacted over the past few decades [27], which have improved the ecosystem function and promoted the forestland ratio from 43.73% (in 2000) to 48.05% (in 2020) (Fig. S1).

Data sources and preparation

The study utilized 7 primary types of data: land use/land cover (LULC), meteorological, remote sensing, soil, topographic, basic geographic information, and socioeconomic statistical data (Table 1). All the data were transformed and resampled to a 100-m resolution.

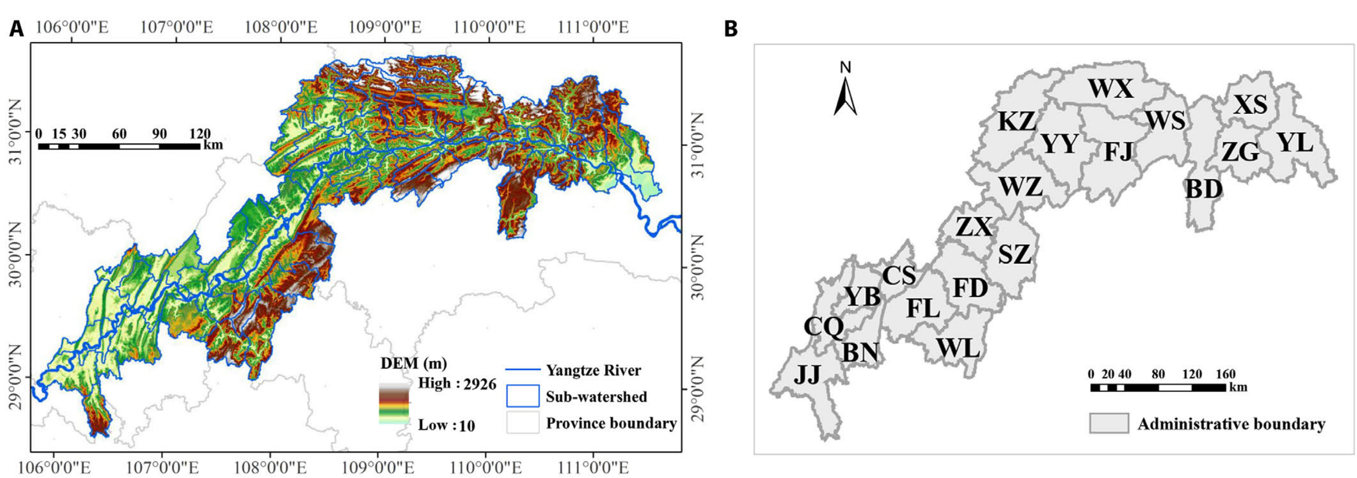

Fig. 1. The location of TGRA (A) and administrative area (B). YL, Yiling; XS, Xingshan; ZG, Zigui; BD, Badong; WS, Wushan; WX, Wuxi; FJ, Fengjie; YY, Yunyang; KZ, Kaizhou; WZ, Wanzhou; ZX, Zhongxian; SZ, Shizhu; FD, Fengdu; WL, Wulong; FL, Fuling; CS, Changshou; YB, Yubei; BN, Banan; CQ, Chongqing; JJ, Jiangjin.

Table 1. Summary of the primary data

Data type	Name	Year	Data source	Data format	Resolution
Land use/cover data	-	2000, 2010, 2020	Resource and Environmental Science and Data Center, Chinese Academy of Sciences (https://www.resdc.cn/)	Raster	30 m
Meteorological data	Temperature Precipitation Solar radiation Sunshine	2000, 2010, 2020	China Meteorological Data Network (https://data.cma.cn)	Shapefile	100 m (Kring interpolate)
Remote sensing data	NDVI	2000, 2010, 2020	NASA MOD13Q1 product (https://www.nasa.gov/)	Raster	250 m (maximum value synthesis https://earthengine.google.com/)
	Nighttime light index	2000, 2010, 2020	Tibetan Plateau Data Center (http://data.tpdc.ac.cn/)	Raster	1,000 m
Soil data	-	2009	China Soil Database (http://vdb3.soil.csdb.cn/)	Shapefile	100 m (Raster conversion)
Topographic data	DEM Slope	-	Geospatial data cloud (http://www.gscloud.cn)	Raster	30 m
Basic geographic information data	-	2017	National Center for Basic Geographic Information (https://www.ngcc.cn/)	Shapefile	-
Socioeconomic statistical data	Food yield	2000, 2010, 2020	Statistical Yearbook of Hubei and Chongqing province	Raster	250 m (NDVI correction method)
	Population		World Population Database (https://www.worldpop.org/)	Raster	100 m
	Water consumption		Water Resources Bulletin of Hubei and Chongqing province	Raster	1,000 m
	GDP		Statistical Yearbook of Hubei and Chongqing province	Raster	1,000 m
	Carbon emission	-	World Population Database (https://www.worldpop.org/)	Raster	100 m

Methods

Research framework

The comprehensive ESP framework is listed as follows (Fig. 2). First, 6 ES supply–demand and their ratios were quantified. Then, one comprehensive ecological risk assessment framework including CSDR, CSDR trend, total supply trend, and supply trade-off is established to evaluate and grade the ecological risk status in TGRA. Next, the ecological sources are determined according to ecological land and area threshold based on the risk grade. Forth, ecological resistance surfaces are identified by modifying nighttime light and land use data. Finally, according to circuit theory, corridors and strategic nodes are further identified to establish a comprehensive ESP.

Selection and quantification of ESs

ESs were selected when they (a) were related to the socioecological features of TGRA and could reveal important ecological issues and (b) aligned with the framework of the Millennium Ecosystem Assessment [28]. Thus, 6 ESs were chosen for evaluation and mapping, namely, 1 cultural service (ecological recreation), 1 supporting service (habitat maintenance), 2 regulating services (soil retention and carbon sequestration), and 2 provisioning services (water yield and food production). Each ES was assessed for the years 2000, 2010, and 2020.

Food production

Food production is crucial for sustaining human life and advancing socioeconomic growth. The supply was evaluated based on the total crop production and crop yield per unit of cultivated area. The normalized difference vegetation index (NDVI) correction method was applied to redistribute the crop production in the county to the grid scale [29]. The demand was defined according to the amount of food consumption including cereals, rice, and beans and calculated as the production of annual main ration intake and population per unit area [30].

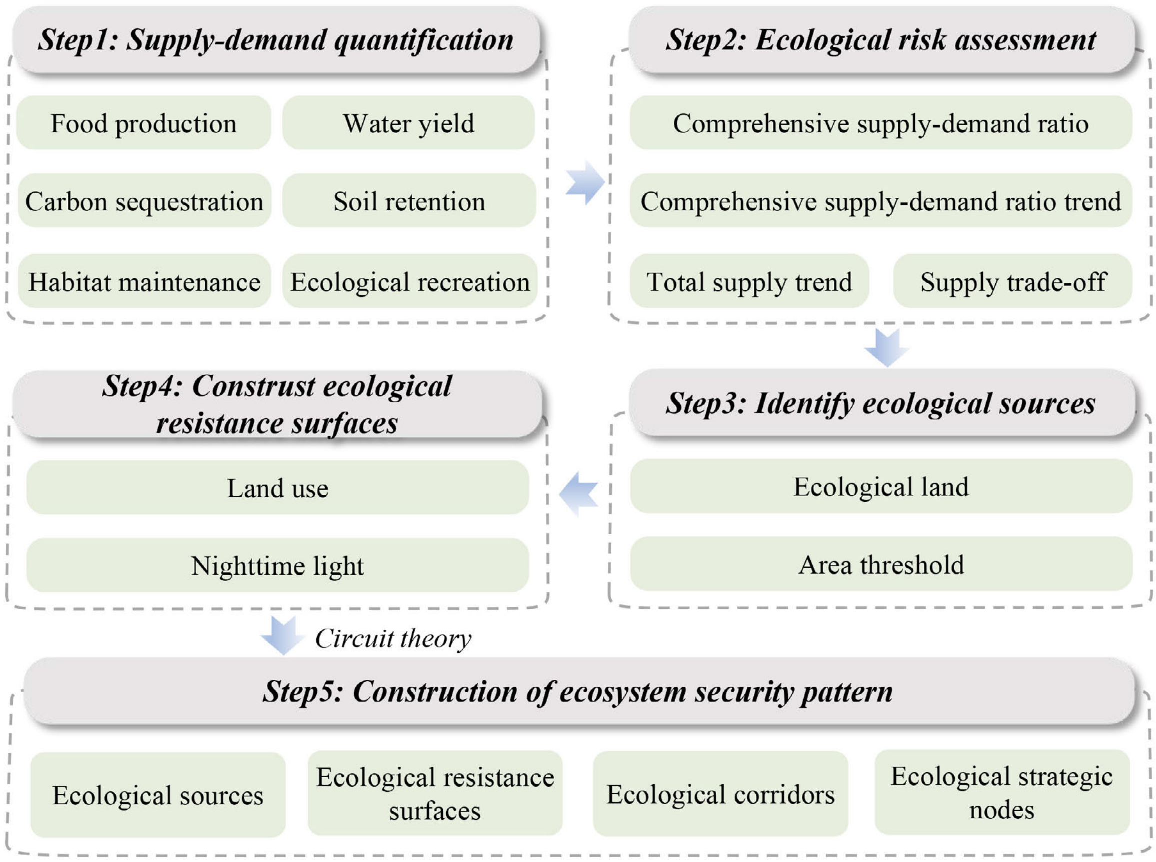

Fig. 2. Comprehensive framework for constructing ESP.

Water yield

Water yield provides essential freshwater resources for human production, daily life, and other activities. Also, it indirectly impacts human well-being by influencing carbon cycles, vegetation, and other processes through hydrological cycles. In this study, water production is the indicator for quantifying water yield supply, referring to the variation between the water resource input and output. The input variables for the InVEST model Water Yield module include precipitation, potential evapotranspiration, biophysical parameter table, root restricting layer depth, and plant available water content (PAWC). PAWC was calculated through soil particle size distribution and organic matter content [21]. The root restricting layer depth was approximated using soil reference depth data from soil surveys. The biophysical parameter table followed the methodologies outlined by Hu et al. [31], and the complete biophysical parameter table is shown in Table S1. The demand is the water resources consumed by human production and living activities within specific spatial contexts [19]. Using the water quota method, we categorized water demand in TGRA, including residential water use, industrial and economic development water use, and agricultural irrigation water use (Table S2). This categorization was integrated with population density, land use, and gross domestic product (GDP) to evaluate the spatial pattern of the demand across TGRA [21].

Carbon sequestration

Carbon sequestration points to the process by natural vegetation captures and sequesters atmospheric CO_2 through photosynthesis, thereby effectively mitigating the greenhouse effect and contributing to global climate change mitigation [32]. Carbon sequestration supply represents the inherent carbon sequestration capacity of natural ecosystems, which can be quantified using net primary productivity (NPP). Given that vegetation sequesters approximately 1.63 times the amount of carbon per unit of accumulated NPP, NPP was calculated by the Carnegie-Ames-Stanford Approach (CASA) model. The demand denotes the total carbon emissions generated by economic and social activities. This study quantified it using county-level energy-related emission inventories from the China Emission Accounts Dataset (CEADs), which integrated fossil fuel combustion and industrial processes [33]. Since the CEADs database provides carbon emission data only at the county administrative level, we utilized night light index (NLI) data to spatially disaggregate these emissions to grid scale. First, we calculated the total NLI intensity for each county and constructed a linear regression model without an intercept term to correlate NLI intensity to the reported carbon emissions. This approach produced county-specific emission calibration coefficients (Table S3), which were subsequently used to estimate grid-scale carbon emissions through fit models.

Soil retention

Soil retention supply points to the ability to limit soil erosion, intercept sediment, and reduce silt in rivers, lakes, wetlands, and reservoirs. In this study, we quantified soil retention supply using the revised universal soil loss equation (RUSLE) model. The demand represents the actual and potential losses caused by soil erosion that humans seek to prevent. Since actual soil erosion risks are undesirable, this study quantified demand based on soil erosion intensity: Higher erosion risk indicates a greater demand for soil retention [34].

Habitat maintenance

The Habitat Quality module was employed to evaluate habitat maintenance supply by integrating land use type-specific sensitivities and intensities to threat factors [35]. To capture the spatial heterogeneity of habitat maintenance, secondary-level land use classification data were utilized. Considering the local features of TGRA, this study chose dry land, urban residential land, paddy field, bare land, other construction land, and urban land as the primary threat factors. Following relevant research [36], we determined habitat suitability scores and sensitivity coefficients for every land cover in relation to these threats (Table S4), as well as the maximum influence distances, weighting factors, and spatial decay types for different threat sources (Table S5). The demand, depending on the biology needs for habitats and the human needs for biodiversity, was related to the socioeconomic indicators, namely, distance from the city, population density, and GDP.

Ecological recreation

Ecological recreation supply, which refers to the capacity of ecosystems providing recreational opportunities without direct human input, was evaluated based on the inherent recreation potential. Considering that it was difficult to obtain the tourist data at the grid scale, this study used local residents to quantify ecological recreation demand based on relevant methods in existing studies [37]. High population density often lacks sufficient green space and has a theoretically more demand for ecological recreation. Therefore, population density is selected as a proxy for demand [38]. To account for spatial variations in willingness to pay and socioeconomic payment capacity across regions, an economic adjustment coefficient was incorporated to standardize the assessment of ecological recreation demand [37].

All ESs were resampled to 100-m resolution. The detailed methods for calculation process to quantify ESs were presented in Table S6. To eliminate the impact of dimensional differences among various ESs, a min–max normalization was applied to the ESs before the analysis.

$$ES_{std} = \frac{\left(ES_{obs} - ES_{min}\right)}{\left(ES_{max} - ES_{min}\right)} \quad (1)$$

where ES_{std} represents normalized value of the ES; ES_{obs} refers to the actual value of the ES; and ES_{max} and ES_{min} refer to the maximum and minimum values of the ES, respectively.

Ecological risk assessment

Ecological risk assessment was mapped with the spatial overlay including CSDR, CSDR trend, total supply trend, and trade-off. The risk grade was shown in Table S7.

The current situation and trend of CSDR

SDR shows the associations between nature supply and human demand, and also the spatial mismatches and congruencies of supply–demand [39].

$$SDR_x = \frac{S_x - D_x}{\left(S_{max} + D_{max}\right)/2} \quad (2)$$

where SDR_x is the supply–demand ratio of various ES types in the grid cell x; S_x and D_x denote supply and demand of various ES types in the grid cell x, respectively; and S_{max} and D_{max} represent maximum values of the supply and demand of various ES types, respectively. "$(S_{max} + D_{max})/2$" represents the average level of max overall supply and demand, aiming to mitigate scale effects and balance the influence of extreme values, thereby facilitating spatial comparison [39].

The CSDR represents the total state of supply–demand and spatial heterogeneity of supply–demand matches [9].

$$CSDR = \frac{1}{n}\sum_{i=1}^{n} ESDR_i \quad (3)$$

where n represents the type number of ESs, equal to 6, and $ESDR$ refers to the SDR_i of the ith ES.

The CSDR trend reflects the relative variations in supply and demand across particular spatiotemporal scales, and is calculated by the differences of CSDR values in different years [16].

Total supply trend

The total supply trend shows the absolute change in the overall ES supply capacity within a defined temporal interval [16].

$$S_t = S_m - S_n \quad (4)$$

where S_t represents the difference of the total supply of ESs in different years. S_m and S_n denote the total supply of ESs in m and n years, respectively.

The total supply can be expressed as the multi-year standardized mean of ESs [9].

$$S_j = \frac{1}{n}\sum_{i=1}^{n} \frac{S_{i,j} - S_{i,min}}{S_{i,max} - S_{i,min}} \quad (5)$$

where S_j represents the relative total supply of 6 normalized ESs in the ith raster cell. $S_{i,j}$ represents the supply of the jth ESs in the ith raster. $S_{i,min}$ and $S_{i,max}$ represent the minimum and maximum values, respectively, of the ith across multiple years for the ES raster.

Trade-off of ES supply

The root mean square deviation was applied to quantitatively analyze the trade-offs among ESs [40]. This method extended conventional negative correlation analysis by quantifying the mean diversity divergence between the standard deviations of individual ES and the mean ES deviation [41].

$$RMSD = \sqrt{\frac{1}{n-1} \times \sum_{i=1}^{n}\left(ES_i - \overline{ES}\right)^2} \quad (6)$$

where n denotes the number of ESs and ES_i denotes the normalized value of the ith ES. $\overline{ES}$ denotes the mean value of nth ESs. Since the theoretical range of $RMSD$ is 0 to 1, following Zeng et al. [42], synergistic relationship among ESs is identified when the $RMSD$ value is $\leq$0.2, whereas an $RMSD$ value of >0.2 represents trade-off relationship [42].

Construction of ESP

Recognition of ecological sources

According to the ecological risk assessment results and to ensure ecosystem sustainable development, the original ecological sources were recognized by the areas with a safe ecological risk level. Then, ecological land (i.e., grassland, water body, and forestland) within the safe areas was extracted and the continuous ecological land was divided into ecological patches. Next, taking 2 km^2 as the step size based on the average size of ecological patches in TGRA and using piecewise linear regression, the total area and the amount of patches smaller than the least patch area threshold were assessed to determine the optimal threshold. Only ecological patches exceeding the threshold for the least area were retained as the final ecological sources [9].

Recognition of ecological resistance surfaces

Resistance values were determined owing to the relative suitability of diverse land cover: forestland (1), grassland (10), cropland (30), water body (50), bare land (300), and construction land (500) [43]. Nighttime light data, a common indicator of human activity intensity, has been widely used in ecological risk assessment and resistance surface recognition [43]. Higher human activity intensity leads to greater resistance to ecological processes. Therefore, base resistance surface derived from land use data was further corrected using nighttime light data [44].

$$R_{xj} = \frac{NLI_x}{NLI_j} \times R_j \quad (7)$$

where R_{xj} denotes the corrected resistance value of the xth raster of class j land cover. R_j denotes the basic resistance value of the jth type of land cover. NLI_x represents the nighttime light index of the xth raster of class j land cover. When $NLI_x = 0$, R_{xj} is set to R_j. NLI_j represents mean nighttime light index of the xth raster of class j land cover.

Recognition of ecological corridors

The Linkage Mapper toolbox was utilized to determine key corridors and potential corridors [3]. First, every ecological source was termed a circuit connection point, and cost-weighted distance (CWD) to the nearest source for every pixel was calculated across the resistance surface. Next, by overlaying the CWD raster with ecological sources, the least-cost distance (LCD) between sources was calculated and the corresponding paths with minimal cumulative resistance were identified as least-cost paths, which represent key ecological corridors. Because ecological processes (e.g., energy flow and species migration) occurred across spatially continuous areas rather than linear paths, we further generated potential corridors by iteratively applying CWD truncation thresholds (ranging from 1,000 to 9,000 in increments of 1,000) within the Linkage Mapper software [45].

Recognition of ecological strategic nodes

Pinch points are vital nodes in ecological processes, and the loss of pinch points can severely compromise regional connectivity, which makes them as priority targets for protection [15]. Barrier points refer to areas within landscape that hamper species movement among ecological sources. Restoring or removing these regions could effectively decrease cumulative resistance and notably enhance interconnection [45]. The Linkage Mapper software was used to identified them. Based on the ecological corridor construction, the Pinchpoint Mapper tool was used to iteratively calculate current flow. For each ecological source, 1-A current was injected while grounding other sources, generating cumulative current density layers. Pinch points were the regions exhibiting the highest current values. Barrier points were recognized by the Barrier Mapper tool. The tool operates under the hypothesis that ecological restoration of a specific area would reduce resistance, thereby decreasing the LCD of optimal pathways passing through the restored region. A moving window approach was applied with 5 search radii (200, 400, 600, 800, and 1,000). The improvement in landscape connectivity post-restoration was quantified by the connectivity improvement value per unit distance, defined as the ratio of the difference in LCD before and after restoration to the search radius [46].

$$IS = \frac{LCD_0 - LCD_1}{D} \quad (8)$$

where IS represents the improvement coefficient and a larger coefficient indicates a higher degree of regional connectivity enhancement. LCD_0 represents the initial LCD value (baseline connectivity state). LCD_1 represents the post-obstacle removal LCD value (connectivity after eliminating barriers). D represents the search radius.

Results

Spatiotemporal variations of ES supply and demand

All the 6 ES supply and demand exhibited clear spatiotemporal heterogeneity (Figs. S2 to S4). The supply of carbon sequestration, habitat maintenance, soil retention, and ecological recreation was notably higher in the eastern regions than in the western regions due to the less human interference and higher vegetation coverage. However, the supply of water yield was exactly the opposite (Fig. S2). The urban areas with high economic development and dense population were high-demand hotspots and also resulted to supply–demand imbalance for food production, water yield, carbon sequestration, habitat maintenance, and ecological recreation, especially around the central districts of Chongqing City (Figs. S3 and S4). However, the high-value regions with SDR of soil retention were situated in the eastern forestland owing to the high supply and low demand. Temporally, the supply of carbon sequestration and ecological recreation increased from 2000 to 2020 because of the implementation of the Grain-for-Green Program, whereas that of food production and habitat maintenance decreased with increased population density. The supply of water yield and soil retention decreased first and increased later, and the supply of water yield significantly improved from 2010 to 2020 specially in the east (Fig. S2). Except for soil retention, the demand for other ESs was increasing (Fig. S3) and the hot demand areas were expanding with social economy development, which resulted the supply–demand imbalance was also gradually expanding with hot demand areas expanding (Fig. S4).

Ecological risk assessment

The situation and trend of CSDR

The situation and trend of CSDR presented obvious spatial heterogeneity (Fig. S5). In the regions with high vegetation coverage, the CSDR was in surplus. In the central areas, it was balance; however, the deficit areas were distributed near the cities with high population density and demand. The CSDRs were 0.20, 0.19, and 0.19 in 2000, 2010, and 2020, respectively, which were relatively stable on the whole, indicating that the supply in most areas in TGRA could meet the demand. The obvious increasing areas of the CSDR were principally established in the central–western regions, while the decreasing regions were distributed near the urban areas due to the increasing demand from 2000 to 2010. The CSDR trend showed bipolar change from 2010 to 2020, showing that the CSDR was improved in most areas but obviously decreased in the urban areas.

Total supply trend and trade-off

The total supply trend and trade-off showed significant spatiotemporal heterogeneity (Fig. S6). The average of total supply was 0.42, 0.41, and 0.45 in in 2000, 2010, and 2020, respectively, showing decreased first and then rapid increase (Fig. S7). The high values were primarily located in the eastern and central–southern regions, while the low values were predominantly situated in the urbanization areas that increased with time. The areas of total supply decreased in the east, accounting for 55.98% within the whole area of TGRA, and it increased in the central areas, accounting for 44.02% from 2000 to 2010 (Fig. S6A). However, the total supply in most areas showed an increasing trend from 2010 to 2020 (Fig. S6B). The average RMSD was 0.36 and 0.33 in 2010 and 2020, respectively. The zones characterized by strong trade-offs were dominantly situated in the eastern and central–southwestern areas, whereas areas with general trade-offs were distributed in the urbanized zones of Chongqing City and the central–northeastern regions in 2010 (Fig. S6C). The trade-offs in central and eastern areas weakened in 2020 (Fig. S6D).

Spatial pattern of ES risk

Overall, the spatial pattern of ES risks had significant differences (Fig. 3). The areas with near under-supply had the largest segment predominantly located in the central–eastern regions in 2010 (Fig. 3A); however, areas with safe level in 2020 were dominated (Fig. 3B). Compared with the areas of risk level between 2010 and 2020, the area with unchanged, reduced, and increased risk levels accounted for 52.06%, 18.54%, and 29.40% within the whole area, respectively (Fig. 3). Thus, the regional ecological risk tends to be safe with increasing risk level, but the main urban zones of Chongqing City with high population density and developed economy faced severe ecological risk and the risk coverage showed expansion.

Establishment of ESPs

Recognizing the ecological sources

The original ecological sources were recognized according to the areas exhibiting a safe ecological risk level in 2020. A total of 95,933 original ecological sources with 24,002.16 km^2 were recognized. The patches <5 km^2 were excluded according to the minimum patch area threshold to ensure ecosystem stability (Fig. 4A). Finally, the identified ecological sources covered 18,232.59 km^2, representing 31.49% of TGRA, and they were predominantly composed of forestland (85.36%), followed by grassland (14.19%) and water bodies (0.45%). Perhaps, the continued implementation of the Grain-for-Green Project since 2002 has contributed to a sustained increase in forest cover within the region. By 2010, the proportion of land use as forest had increased by 4.4% compared with 2000 (Fig. S1 and Table S8). By 2020, large-scale ecological restoration of sloping cropland had been achieved across TGRA, with approximately 776.04 km^2 of cropland converted to forestland and grassland (Table S9). Meanwhile, the ecological sources are largely situated in the eastern zones with good ecological quality and rich forest and grass ecological resources and some areas on the southern side of the Yangtze River (Fig. 4B). However, a total of 904.66 km^2 of other land cover were converted into construction land (Table S9), with the most significant expansion observed in the urbanized zones of Chongqing City. This rapid urban expansion has contributed to the relatively sparse pattern of ecological sources in the vicinity of Chongqing City.

Establishing the ecological resistance surface

The basis resistance surface exhibited elevated values in the western and northern zones, while the eastern and southern zones showed lower values (Fig. 5A). Specially, the low value of the resistance surface was distributed consistently with the ecological sources; however, the high value of resistance surface was distributed near the town. The rapid urbanization and industrialization led to the crowding of some ecological land, which influenced the ecosystem process and functional connectivity. As shown in Fig. 5B, the value of modified resistance surface was consistent with the basis resistance surface in the spatial distribution. The highest and lowest resistance values were 2,874.42 and 0.01,

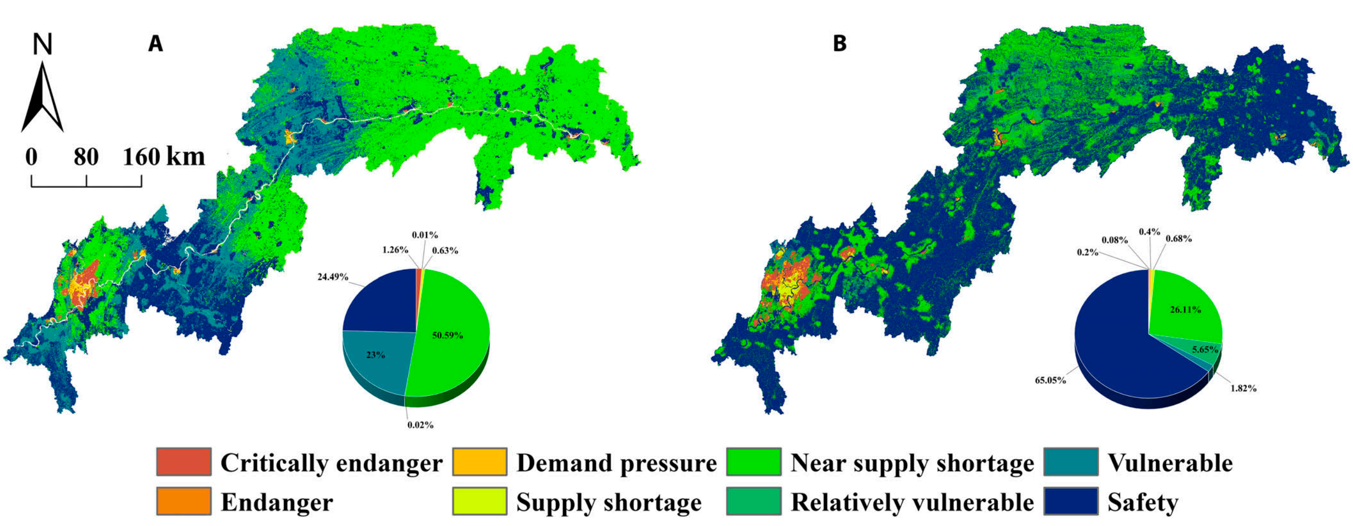

Fig. 3. Spatial pattern of ecological risk in 2010 (A) and 2020 (B).

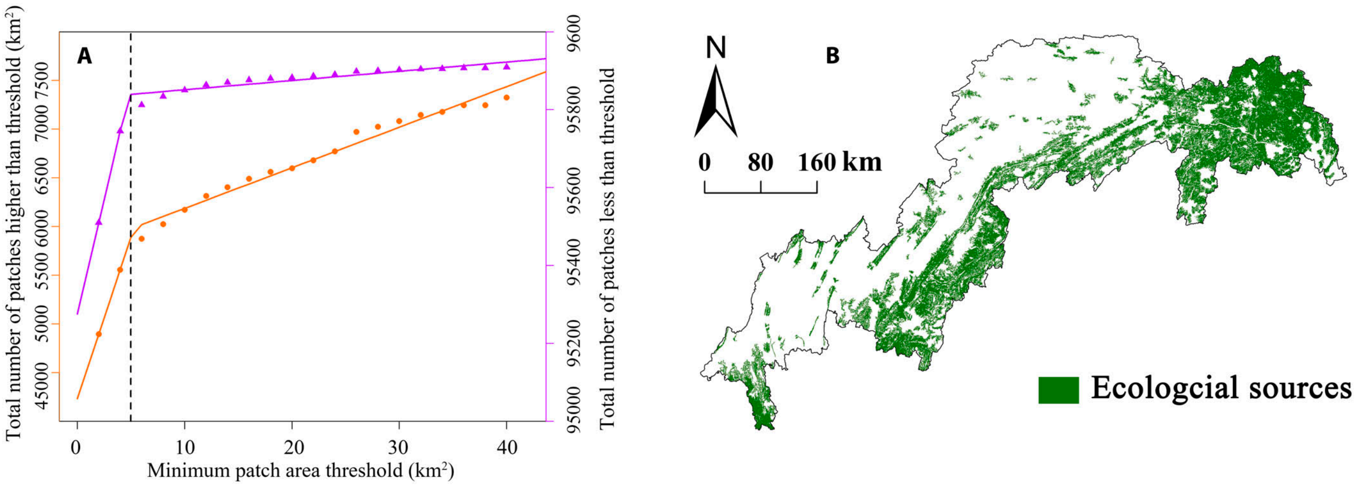

Fig. 4. The overall area and number of ecological patches under different minimum patch area threshold (A) and spatial pattern of ecological sources (B).

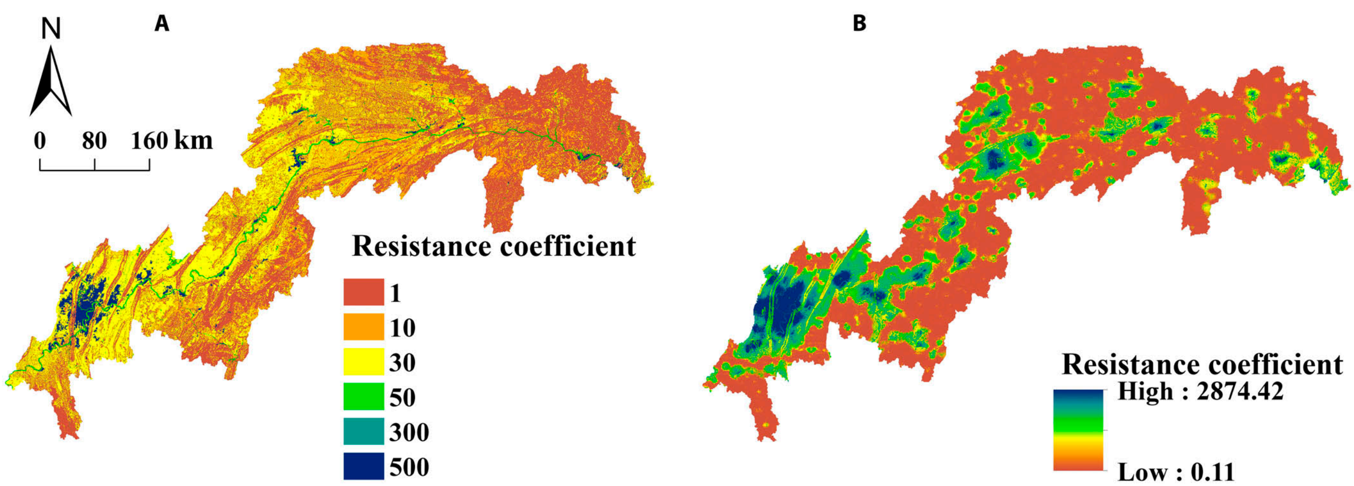

Fig. 5. Spatial pattern of basic resistance surfaces (A) and modified resistance surfaces (B).

respectively, with a mean modified resistance of 29.38. In comparison with the basic resistance values, which spanned from 1 to 500, the modified resistance surface exhibited a superior precision and greater differentiation.

Extracting the ecological corridors

Two hundred sixty-six key ecological corridors, having an overall length of 2,517.83 km, were extracted (Fig. 6A). Overall, these corridors formed a network that connected the ecological sources, thereby providing pathways for the flow of energy and migration of species. Based on natural breakpoint method, the key ecological corridors were classified into 230 small resistance corridors, 28 medium resistance corridors, and 8 large resistance corridors (Fig. 6B). Small resistance corridors were mostly distributed in the central–eastern zone, and large resistance corridors were situated in the urbanized zones of Chongqing City, indicating that construction land reduced the ecological sources and also hindered the corridor connectivity. The potential ecological corridors with the area of 13,048.81 km^2 were further recognized (Fig. 6C) based on the CWD cutoff value (CWD cutoff value = 3,000) (Fig. S8). The potential ecological corridors cross-overlapped in the central areas and had a wide range; however, they were relatively narrow in the east due to urbanization.

Recognizing the ecological strategic nodes

Approximately 195 ecological pinch points were recognized according to the peak cumulative current values within high-resistance (red) regions (Fig. 7A). These pinch points were mostly distributed in the western regions, characterized by high landscape resistance dominated by cropland, construction land, and fragmented forestland. The improvement factor was divided into low, medium, and high grades according to the natural breakpoint method, and the high grade regions represented the barrier points (approximately 94) with 1,151.52 km^2 (Fig. 7B). The barrier points with an area of 285.96 km^2 had spatial overlap with the potential corridors, indicating that some barrier points may lead to the fracture risk of corridors due to high local resistance value. These barrier points were largely founded in the central–eastern regions and western regions, and cropland with 501.09 km^2 was the predominant land cover. However, the forestland was also widely situated in the central–eastern regions, indicating that the Grain-for-Green Program could continue to be implemented to heighten the landscape connectivity in these zones.

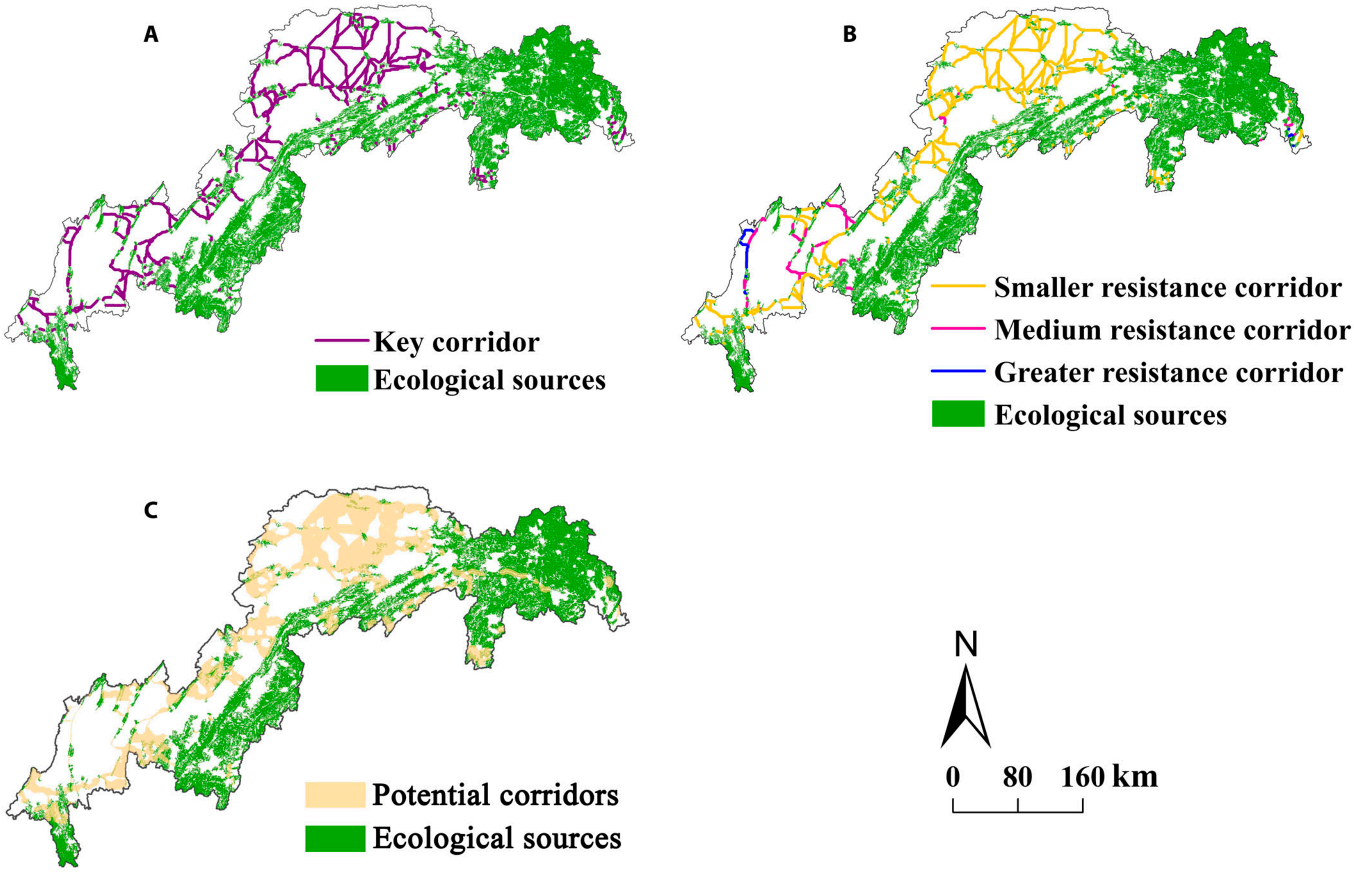

Fig. 6. Spatial pattern of corridors. (A) Key corridors. (B) Key corridors with different resistance levels. (C) Potential corridors.

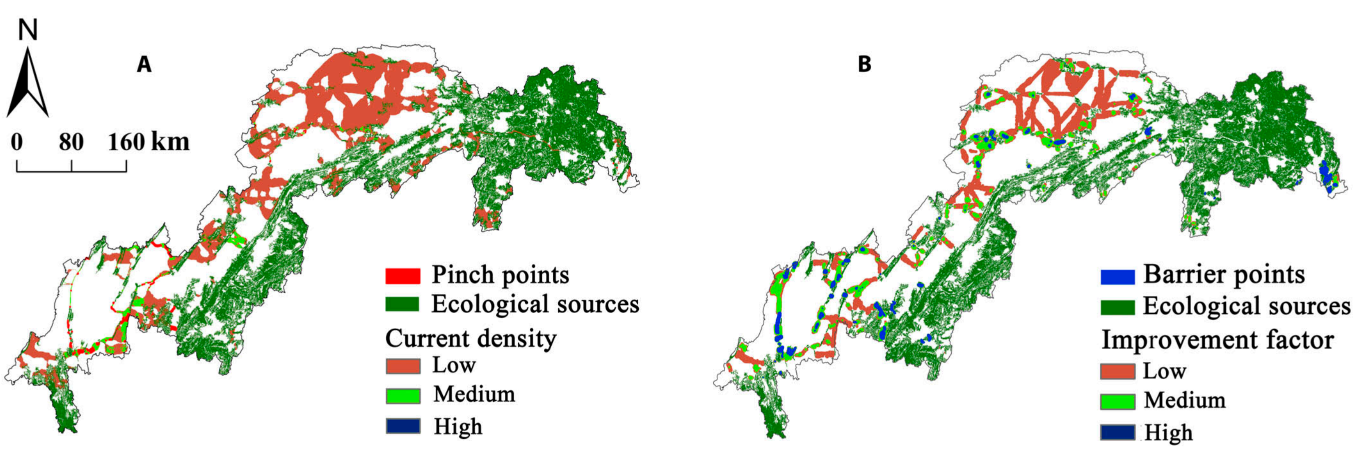

Fig. 7. Spatial pattern of ecological strategic nodes. (A) Pinch points. (B) Barrier points.

Discussion

Impacts of ES supply–demand balance on constructing comprehensive ESP

Integrating supply–demand balance into ESP is crucial for sustainable development [3]. Nature and human elements both affect the spatiotemporal distribution of supply and demand [6]. We found that supply and demand in TGRA had an urban–rural gradient; specifically, there was generally excess demand in urban areas and surplus supply in more remote natural regions. Specifically, the eastern mountainous regions, characterized by dense forest cover, exhibited the higher supply of water yield, carbon sequestration, soil retention, and ecological recreation [47]. Meanwhile, the urban areas showed supply–demand mismatch because of high demand related to high population density and limited supply ecological conditions [6]. Therefore, different from the traditional focus on ES importance or sensitivity, this study was grounded in the perspective of ecological risk assessment and ESP construction, integrating both ecosystem characteristics and human welfare demands, and places greater emphasis on the critical role of supply–demand matching.

Integrating dynamic trends into supply–demand assessments aims to enhance the long-term provision of benefits to humans. On the one hand, current status alone could underestimate ecological risks [24]. To illustrate, carbon sequestration supply in the central and eastern regions in 2020 decreased compared to 2010 (Fig. S2), but it still showed supply–demand balance (Fig. S4), which indicated that the ecosystems may be unable to provide sufficient supply and could face long-term degradation risks. On the other hand, the comparison of ecological risk assessments between 2010 and 2020 revealed that there were prominent variations in the distribution patterns, which showed that ES supply during random time periods may be susceptible to natural factors, or delayed responses of ecosystems to ecological projects could also influence the spatial pattern of both the total supply trend and CSDR trend. Thus, it is vital to estimate supply–demand based on a long-term and continuous time to enhance the precision of ecological source recognition for constructing ESP.

The results illustrate the accuracy of supply–demand balance on the ecological source identification by coupling supply and demand. The ecological sources are predominantly situated in the eastern areas and the southern side of the Yangtze River with high supply and surplus CSDR; however, in urbanized zones with high population density and demand, deficit supply, decreasing CSDR, and high ecological risks, the increasing construction land reduced the ecological sources. Fair allocation of ecological resources and the mitigation of spatial imbalances in ESs represent key pathways for addressing ecological injustice [3]. As an illustration, Shi et al. [38] highlighted that the protection of urban green spaces should prioritize central urban areas and inner suburbs, rather than focusing solely on the peripheral suburbs. Therefore, the priority protection areas according to ES supply–demand balance can reduce the risk of more severe mismatches in rapidly urbanizing regions [3].

Optimized management policies in TGRA based on ESP

ESP provides a fundamental framework for identifying priority conservation areas and establishing an integrated and connected ecological network that supports regional ecological stability and long-term sustainability [17]. The study discusses the control strategy of ESP from 3 aspects: preservation of core ecological sources, establishment of diversified corridors, and protection and restoration of key strategic nodes (Fig. 8).

The ecological sources, primarily covered by forestland, were vital areas to ensure the stability of TGRA and carried the important ecological functions of habitat maintenance, soil retention, and carbon sequestration. On the whole, the ESs in

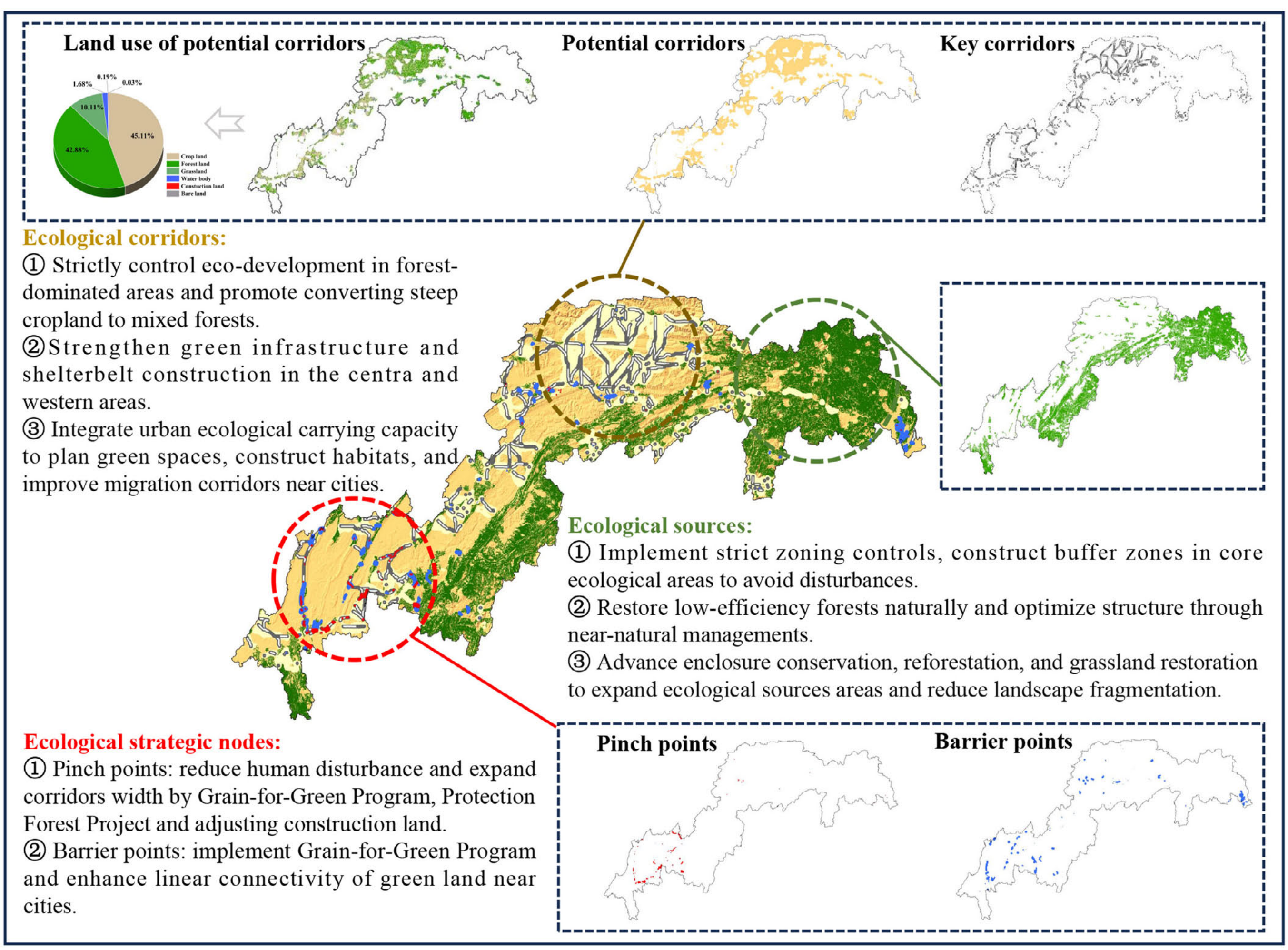

Fig. 8. Management measures for different regions based on ESP.

these areas showed surplus supply and the ecological risk level is safe in the short term. Conservation and restoration of ecological sources is the foundation of maintaining regional ecological security [7]. First, we could implement strict zoning controls and construct buffer zones in core ecological areas to avoid disturbances. Meanwhile, restore low-efficiency forests naturally and optimize structure through near-natural managements. Additionally, advance enclosure conservation, reforestation, and grassland restoration to expand ecological sources areas and reduce landscape fragmentation.

Ecological corridors connect the region into an organic whole by constructing the network connectivity among the ecological sources [10]. The ecological corridor number in our study was relatively more than the study of Peng et al. [48] and Sun et al. [49] in TGRA. The main reason was that we incorporated small patches grounded on the average size of ecological patches in TGRA and threshold when identifying ecological sources, which enhanced the connectivity of the region. Moreover, in the eastern area, the proportion of forestland was relatively high, but the existence of cropland causes obstacles to the connectivity of ecological corridors (Fig. 8). Thus, these areas require strict regulation of ecological development and the promotion of converting steep cropland to mixed forests. The ecological corridors distributed in the central–western regions occupy a significant proportion of cropland, and the cropland shows concentrated distributions; therefore, the establishment of green infrastructure requires further strengthening by connecting the ecological land and non-ecological land through shelterbelt to improve the quality of non-ecological land. Meanwhile, urban ecological carrying capacity should be integrated into planning to develop green spaces, build habitats, and expand migration corridors near cities.

The strategic nodes are not only key points connecting the ecological sources but also ecological fragile points susceptible to external disturbances [15]. Pinch points were high-density areas where the ecological processes occur [14] and mostly distributed around the core urban zones of Chongqing City and many of them near the barrier points. Furthermore, as ecological corridors expanded, the number of pinch points also increased. Thus, it is necessary to reduce human disturbance and enlarge corridor widths via the Grain-for-Green Program, the Protection Forest Project, and the adjustment of construction land. Barrier points are mostly distributed in the regions with dense human activities, and their land use types are mostly cropland, so Grain-for-Green Program is implemented and linear connectivity of green land near cities is enhanced.

Limitations and applicability of the ESP framework

The ESP framework in this research is universally applicable in the regional scale. However, when applying it in smaller scales or regions with homogeneous ecosystems (e.g., plain agricultural areas), may need to pay attention to resistance surface values. In this context, more precise data (e.g., socioeconomic, land use, and climate factors) are needed to reflect the ecological heterogeneity. In addition, when quantifying the demand of ecological recreation, this study focused on local residents and overlooked the tourist demand. Future research could consider integrating supplementary data sources, such as local tourism statistics, to better identify the recreational behaviors of different groups and thereby improve the accuracy of ecological recreation service assessments.

Conclusion

The construction of ESPs provides a scientific basis for recognizing priority conservation regions and enhancing regional ecological security. A comprehensive ESP framework was identified by integrating supply–demand balance, ecological risk, and circuit theory. This ESP identified 140 ecological sources, 260 key corridors, 13,048.81 km^2 potential corridors, 195 pinch points, and 94 barrier points. The ecological sources were principally founded in the eastern areas and some regions on the southern side of the Yangtze River with higher supply and lower ecological risk and trade-off level, which were the basis for ensuring regional ecological security and continuously delivering ESs to surrounding areas. The weak supply areas and strategic nodes were predominantly distributed in the urbanized zones with high population density and demand (especially in Chongqing City). Reducing human disturbance and expanding corridor width by Grain-for-Green Program were the important measure to regulate the supply capacity and maintain the regional ecological stability. The ecological corridors were dominantly founded in eastern and central areas, and the existence of cropland caused obstacles to their connectivity. Thus, it is necessary to strictly control ecological development in these areas and promote the conversion of steep cropland into mixed forests. The findings could provide important support for regional ecological constructions and governance policies in TGRA.

Acknowledgments

Funding: This work was supported by the National Key Research and Development Program of China (2023YFE0112804 and 2023YFF1305205), the Fundamental Research Funds for the Central Non-profit Research Institute of Chinese Academy of Forestry (CAFYBB2023MA011), and the National Natural Science Foundation of China (32301669).
Author contributions: R.H.: Conceptualization, data curation, and writing—original draft. H.Z.: Data curation and writing—original draft. J.Y.: Software. M.G.: Conceptualization, data curation, writing—review and editing, and funding acquisition. C.L.: Methodology, resources, and funding acquisition. L.L.: Writing—review and editing and funding acquisition. W.X.: Methodology and resources.
Competing interests: The authors declare that they have no competing interests.

Data Availability

Data will be made available on request.

Supplementary Materials

Figs. S1 to S8
Tables S1 to S9

References

1. Costanza R, d'Arge R, de Groot R, Farber S, Grasso M, Hannon B, Limburg K, Naeem S, O'Neill RV, Paruelo J, et al. The value of the world's ecosystem services and natural capital. *Nature*. 1997;387:253–260.
2. Xia HX, Yue WZ, Xu JR, Xiong JH, Hu HW, Wang TY, Wu X. Integrating ecosystem services into ecological zoning

management: Insights from the Shan-Shui Initiative in China. *Ecosyst Health Sustain*. 2025;11:0368.
3. Jia QQ, Jiao LM, Lian XH, Wang WL. Linking supply-demand balance of ecosystem services to identify ecological security patterns in urban agglomerations. *Sustain Cities Soc*. 2023;92:Article 104497.
4. Wu JS, Fan XN, Li KY, Wu YW. Assessment of ecosystem service flow and optimization of spatial pattern of supply and demand matching in Pearl River Delta, China. *Ecol Indic*. 2023;153:Article 110452.
5. Lyu X, Li XB, Wang K, Cao WY, Gong JR, Wang H, Lou AR. Linking regional sustainable development goals with ecosystem services to identify ecological security patterns. *Land Degrad Dev*. 2022;33(18):3841–3854.
6. Shen JS, Li SC, Wang H, Wu SY, Liang Z, Zhang YT, Wei FL, Li S, Ma L, Wang YY, et al. Understanding the spatial relationships and drivers of ecosystem service supply-demand mismatches towards spatially-targeted management of social-ecological system. *J Clean Prod*. 2023;406:Article 136882.
7. Shu R, Ma GQ, Zou YB, Guo N, Su HZ, Zhang GQ. Bibliometric analysis of ecological security pattern construction: Current status, evolution, and development trends. *Ecol Indic*. 2024;169:Article 112754.
8. Li JM, Liang LE, Chao Y, Wang XH, Qiu MM, Luo PP, Zhu YH. Construction of the ecological security pattern of Mu Us sandy land on the basis of the "Source-Resistance-Corridor" theory. *Ecol Indic*. 2025;171:Article 113162.
9. Jiang H, Peng J, Dong JQ, Zhang ZM, Xu ZH, Meersmans J. Linking ecological background and demand to identify ecological security patterns across the Guangdong-Hong Kong-Macao Greater Bay Area in China. *Landsc Ecol*. 2021;36:2135–2150.
10. Dong X, Wang F, Fu MC. Research progress and prospects for constructing ecological security pattern based on ecological network. *Ecol Indic*. 2024;168:Article 112800.
11. Han PY, Hu HZ, Jiang MT, Wang M. Construction of wetland ecological security pattern in Wuhan metropolitan core area considering wetland ecological risk. *Land*. 2024;13(9):1407.
12. Huang YC, Zhang JB, Zhang PY, Chen Z, Zhang XY, Lu R, Li MF, Xing GR, Song YP. Construction and optimization of ecological security pattern based on landscape ecological risk assessment in the affected area of the Lower Yellow River. *Front Ecol Evol*. 2023;11:Article 1271352.
13. Zhang LQ, Peng J, Liu YX, Wu JS. Coupling ecosystem services supply and human ecological demand to identify landscape ecological security pattern: A case study in Beijing-Tianjin-Hebei region, China. *Urban Ecosyst*. 2016;20:701–714.
14. Li XB, Li X, Lyu X, Dang DL, Wang K, Zhang CH, Cao WY. Linking ecological and social systems to promote regional security management: A perspective of ecosystem services supply-flow-demand. *Ecol Indic*. 2023;156:Article 111124.
15. Wu TK, Lu SW, Ding YC. Ecological security evaluation system integrated with circuit theory for regional ecological security pattern construction: A coordinated study of Chang-Zhu-Tan metropolitan area in China. *Land*. 2025;14(2):257.
16. Wang ZZ, Zhang LW, Li XP, Li YJ, Fu BJ. Integrating ecosystem service supply and demand into ecological risk assessment: A comprehensive framework and case study. *Landsc Ecol*. 2021;36:2977–2995.
17. Peng J, Pan YJ, Liu YX, Zhao HJ, Wang YL. Linking ecological degradation risk to identify ecological security patterns in a rapidly urbanizing landscape. *Habitat Int*. 2018;71:110–124.
18. Schirpke U, Candiago S, VigL LE, Jäger H, Labadini A, Marsoner T, Meisch C, Tasser E, Tappeiner U. Integrating supply, flow and demand to enhance the understanding of interactions among multiple ecosystem services. *Sci Total Environ*. 2019;651:928–941.
19. Burkhard B, Kroll F, Nedkov S, Mueller F. Mapping ecosystem service supply, demand and budgets. *Ecol Indic*. 2012;21:17–29.
20. Gao X, Guo ZY, Zhang MM, Liang XY, Zhao MR, Qin L. Ecological source identification and ecological security pattern construction from the perspective of ecosystem service supply and demand: A case study of Baiyangdian Basin in China. *Environ Dev Sustain*. 2024;27:22947–22970.
21. Gou MM, Li L, Ouyang S, Wang N, La LM, Liu CF, Xiao WF. Identifying and analyzing ecosystem service bundles and their socioecological drivers in the Three Gorges Reservoir Area. *J Clean Prod*. 2021;307:Article 127208.
22. Dade MC, Mitchell MGE, McAlpine CA, Rhodes JR. Assessing ecosystem service trade-offs and synergies: The need for a more mechanistic approach. *Ambio*. 2019;48:1116–1128.
23. Chen FY, Li L, Niu JQ, Lin AW, Chen SY, Hao L. Evaluating ecosystem services supply and demand dynamics and ecological zoning management in Wuhan, China. *Int J Environ Res Public Health*. 2019;16(13):2332.
24. Huang YT, Cao YR, Wu JY. Evaluating the spatiotemporal dynamics of ecosystem service supply-demand risk from the perspective of service flow to support regional ecosystem management: A case study of yangtze river delta urban agglomeration. *J Clean Prod*. 2024;460:Article 142598.
25. Huang CB, Huang X, Peng CH, Zhou ZX, Teng MJ, Wang PC. Land use/cover change in the three gorges reservoir area, China: Reconciling the land use conflicts between development and protection. *Catena*. 2019;175:388–399.
26. Huang CB, Zhao DY, Deng L. Landscape pattern simulation for ecosystem service value regulation of Three Gorges Reservoir Area, China. *Environ Impact Assess Rev*. 2022;95:Article 106798.
27. Li F, Zhou WZ, Shao ZL, Zhou XY. Effects of ecological projects on vegetation in the Three Gorges Area of Chongqing, China. *J Mt Sci*. 2021;19:121–135.
28. Millennium Ecosystem Assessment. *Ecosystems and human well-being: Current state and trends*. Washington (DC): Island Press; 2005.
29. Wang KP, Gao JR, Liu CH, Zhang YL, Wang CX. Understanding the effects of socio-ecological factors on trade-offs and synergies among ecosystem services to support urban sustainable management: A case study of Beijing, China. *Sustain Cities Soc*. 2024;100:Article 105024.
30. Zhang ZM, Peng J, Xu ZH, Wang XY, Meersmans J. Ecosystem services supply and demand response to urbanization: A case study of the Pearl River Delta, China. *Ecosyst Serv*. 2021;49:Article 101274.
31. Hu YN, Peng J, Liu YX, Tian L. Integrating ecosystem services trade-offs with paddy land-to-dry land decisions: A scenario approach in Erhai Lake Basin, southwest China. *Sci Total Environ*. 2018;625:849–860.
32. Jiang C, Zhang HY, Zhang ZD. Spatially explicit assessment of ecosystem services in China's Loess Plateau: Patterns, interactions, drivers, and implications. *Glob Planet Chang*. 2017;161:41–52.
33. Yuan Y, Bai ZK, Zhang JJ, Huang YH. Investigating the trade-offs between the supply and demand for ecosystem

services for regional spatial management. *J Environ Manag*. 2023;325:Article 116591.
34. Yu J, Yi LW, Xie BG, Li XQ, Li JH, Xiao JY, Zhang L. Matching and coupling coordination between the supply and demand for ecosystem services in Hunan Province, China. *Ecol Indic*. 2023;157:Article 111303.
35. Li JY, Geneletti D, Wang HC. Understanding supply-demand mismatches in ecosystem services and interactive effects of drivers to support spatial planning in Tianjin metropolis, China. *Sci Total Environ*. 2023;895:Article 165067.
36. Chu L, Sun TC, Wang TW, Li ZX, Cai CF. Evolution and prediction of landscape pattern and habitat quality based on CA-Markov and InVEST model in Hubei section of Three Gorges Reservoir Area (TGRA). *Sustainability*. 2018;10(11):3854.
37. Gou MM, Liu CF, Xiao WF, Zeng LX, Li L. Ecological zoning management strategies based on ecosystem service supply and demand. *Terrestrial Ecosyst Conserv*. 2022;2:1–12.
38. Shi YS, Shi DH, Zhou LL, Fang RB. Identification of ecosystem services supply and demand areas and simulation of ecosystem service flows in Shanghai. *Ecol Indic*. 2020;115:Article 106418.
39. Xue CL, Xue LR, Chen JP, Tarolli P, Chen XH, Zhang HQ, Qian JC, Zhou Y, Liu XH. Understanding driving mechanisms behind the supply-demand pattern of ecosystem services for land-use administration: Insights from a spatially explicit analysis. *J Clean Prod*. 2023;427:Article 139239.
40. Bradford JB, D'Amato AW. Recognizing trade-offs in multi-objective land management. *Front Ecol Environ*. 2011;10(4):210–216.
41. Lu N, Fu BJ, Jin TT, Chang RY. Trade-off analyses of multiple ecosystem services by plantations along a precipitation gradient across Loess Plateau landscapes. *Landsc Ecol*. 2014;29:1697–1708.
42. Zeng YL, Gou MM, Ouyang S, Chen L, Fang X, Zhao LJ, Li JX, Peng CH, Xiang WH. The impact of secondary forest restoration on multiple ecosystem services and their trade-offs. *Ecol Indic*. 2019;104:248–258.
43. Gou MM, Li L, Ouyang S, Shu C, Xiao WF, Wang N, Hu JW, Liu CF. Integrating ecosystem service trade-offs and rocky desertification into ecological security pattern construction in the Daning river basin of southwest China. *Ecol Indic*. 2022;183:Article 108845.
44. Gao JB, Du FJ, Zuo LY, Jiang Y. Integrating ecosystem services and rocky desertification into identification of karst ecological security pattern. *Landsc Ecol*. 2020;36:2113–2133.
45. Huang JM, Hu YC, Zheng FY. Research on recognition and protection of ecological security patterns based on circuit theory: A case study of Jinan City. *Environ Sci Pollut Res*. 2020;27(11):12414–12427.
46. Jiao S, Liu YC, Han ZW, Zhou KJ, Hu L, Liu TX. Determining priority areas for land ecological restoration based on ecological network-human disturbance: A case study of Changsha-Zhuzhou-Xiangtan urban agglomeration. *J Nat Resour*. 2021;36(9):2294–2307.
47. Xiao Q, Hu D, Xiao Y. Assessing changes in soil conservation ecosystem services and causal factors in the Three Gorges Reservoir region of China. *J Clean Prod*. 2017;163:S172–S180.
48. Peng CH, Wang YH, Dong JW, Huang C, Yang MQ. Identification of priority areas for ecological restoration in the Three Gorges Reservoir Area, China: The systemic and targeted perspectives. *Land Degrad Dev*. 2025;36(12): 4208–4225.
49. Sun DL, Wu XQ, Wen HJ, Ma XL, Zhang FT, Ji Q, Zhang JL. Ecological security pattern based on XGBoost-MCR model: A case study of the Three Gorges Reservoir Region. *J Clean Prod*. 2024;470:Article 143252.

Ecosystem Health and Sustainability
A SCIENCE PARTNER JOURNAL

Integrating Ecosystem Service Supply and Demand to Construct Regional Ecological Security Patterns

Ruyuan Hu, Haiping Zhao, Jia Yang, Mengmeng Gou, Changfu Liu, Le Li, and Wenfa Xiao

Citation: Hu R, Zhao H, Yang J, Gou M, Liu C, Li L, Xiao W. Integrating Ecosystem Service Supply and Demand to Construct Regional Ecological Security Patterns. *Ecosyst Health Sustain*. 2025;**11**:0457. DOI: 10.34133/ehs.0457

Integrating ecosystem services (ESs) into ecological security patterns (ESPs) provides a comprehensive framework for recognizing critical conservation areas and enhancing regional ecological security. However, previous studies are predominantly based on ES supply, while often not fully considering the supply–demand balance and its dynamic trends. This study proposed a comprehensive framework including comprehensive supply–demand ratio (CSDR), CSDR trend, total supply trend, and trade-off to revise ecological source recognition. Subsequently, ecological resistance surfaces were revised using land use and nighttime light data. Finally, corridors and strategic nodes were further recognized according to circuit theory to establish a comprehensive ESP. Selecting Three Gorges Reservoir Area as a research case, the results show that the ecological sources (18,232.59 km2) are predominantly situated in the eastern regions and parts of the southern bank of the Yangtze River with high supply and low ecological risks and trade-off levels. The low value of the resistance surfaces is distributed consistently with ecological sources, and the high value of the resistance surfaces is distributed near the cities with high population density and demand. Two hundred sixty-six key ecological corridors and 195 pinch points connected the regions into an organic whole and barrier points, with an area of 285.96 km2 overlapping with the potential corridors. These findings offer guidance for regional planning and sustainable development.
Image

View the article online
https://spj.science.org/doi/10.34133/ehs.0457

Ecosystem Health and Sustainability (ISSN 2332-8878) is published by the American Association for the Advancement of Science. 1200 New York Avenue NW, Washington, DC 20005.